MODIFIED CRAMER-RAO LOWER BOUNDS FOR TOA AND SYMBOL WIDTH ESTIMATION. AN APPLICATION TO SEARCH AND RESCUE SIGNALS

V. Bissoli Nicolau[1,2], *M. Coulon*[1], *Y. Grégoire*[3], *T. Calmettes*[4], *J.-Y. Tourneret*[1]

[1] University of Toulouse, INP-ENSEEIHT/IRIT, 2 rue Charles Camichel, BP 7122, 31071 Toulouse Cedex 7, France

[2] TéSA, 14-16 Port Saint-Etienne, 31000 Toulouse, France [3] CNES, 18 Av. Edouard Belin, 31401 Toulouse, France

[4] Thales Alenia Space, 26 Av. Jean-François Champollion, 31037 Toulouse Cedex 1, France

{victor.bissolinicolau, martial.coulon, jean-yves.tourneret}@enseeiht.fr

yoan.gregoire@cnes.fr, thibaud.calmettes@thalesaleniaspace.com

ABSTRACT

This paper focuses on the performance of time of arrival estimators for distress beacon signals which are defined by pulses with smooth transitions. These signals are used in the satellite-based search and rescue Cospas-Sarsat system. We propose a signal model based on sigmoidal functions. Closed-form expressions for the modified Cramér-Rao bounds associated with the parameters of this model are derived. The obtained expressions are easy to interpret since they analytically depend on the system parameters. Simulations conducted on realistic search and rescue signals show good agreement with the theoretical results.

***Index Terms*—** Time of arrival, edge detection, symbol width, modified Cramér-Rao bound, Cospas-Sarsat

1. INTRODUCTION

The international Cospas-Sarsat system [1] is designed to detect and locate distress beacons, providing data to assist search and rescue (SAR) operations. Source localization is currently performed using low Earth orbit (LEO) satellites, through Doppler processing. The actual constellation is gradually being replaced by the satellites from the next generation medium Earth orbit (MEO), which will cover larger areas of Earth surface, permitting almost instantaneous alerts [2]. However, due to higher orbits, the MEO satellites will receive weaker signals and will have to handle smaller Doppler shifts. In this scenario, which is similar to the one used in satellite navigation systems, estimation methods based on times of arrival (TOA) or joint TOA and frequencies of arrival (FOA) are currently investigated [3].

The purpose of this work is to study the performance of time of arrival estimators for Cospas-Sarsat rescue signals. We propose to introduce sigmoidal functions (as in [4, 5]) to model the transitions of the Manchester pulses used in the Cospas-Sarsat system. The main contribution of this paper is then to compute the modified Cramér-Rao bounds (MCRBs) [6] for the parameters of the resulting SAR signals already mentioned. The obtained bounds can be easily interpreted, as they analytically depend on the system parameters.

The paper is structured as follows. Section 2 introduces the proposed signal model whose transitions are modeled by sigmoidal functions. Section 3 derives the MCRBs for estimators of TOA and symbol width for the resulting SAR signals. Simulation results are presented in Section 4. Conclusions and relations with prior works are reported in Sections 5 and 6.

The authors would like to thank Thales Alenia Space and the CNES (French government space agency) for funding.

2. SIGNAL MODEL

According to the distress beacon specifications [7], the SAR signal is a binary phase-shift keying (BPSK) signal where the message is bi-phase level encoded, which is equivalent to a Manchester code. The received signal can be modeled as

$$r(t) = s(t) + w(t) \tag{1}$$

with

$$s(t) = A \exp\left\{ j \left[2\pi\nu t + \beta \sum_{n=0}^{N-1} b_n \, g(t - nT - \tau) \right] \right\} \tag{2}$$

where $w(t)$ is an additive complex white Gaussian noise with two-sided power spectral density (PSD) $2N_0$ (the real and the imaginary part of $w(t)$ have a PSD equal to N_0), A is the signal amplitude, ν is the residual carrier frequency resulting from synchronization errors, N is the number of symbols, β is the modulation index in radians, $\mathbf{b} = \{b_n\}$ is a zero-mean independent and identically distributed (iid) sequence of random variables associated with the information bits, T is the symbol width and τ is the transmission delay. Fig. 1(a) shows the signal phase $\phi(t)$ and Fig. 1(b) illustrates the signal space, where $s_R(t)$ and $s_I(t)$ are the real and imaginary parts of $s(t)$. In order to consider the smooth phase transitions between $-\beta$ and β, we propose the following model for the real pulse $g(t)$

$$g(t) = \frac{1}{2} f_\alpha(t) - f_\alpha(t - T/2) + \frac{1}{2} f_\alpha(t - T) \tag{3}$$

where $f_\alpha(t)$ is a sigmoid function defined as

$$f_\alpha(t) = \mathrm{erf}(\alpha t) = \frac{2}{\sqrt{\pi}} \int_0^{\alpha t} e^{-x^2} dx. \tag{4}$$

The main motivation for using (4) is that the derivative of the error function is a Gaussian pulse, which has a simple Fourier transform.

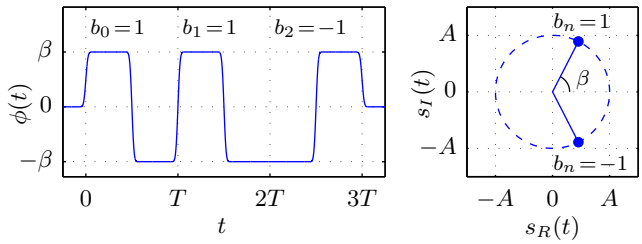

(a) Phase of $s(t)$ for $\mathbf{b} = (1, 1, -1)$. (b) Signal space.

Fig. 1. Illustration of (a) phase and (b) signal space of $s(t)$.

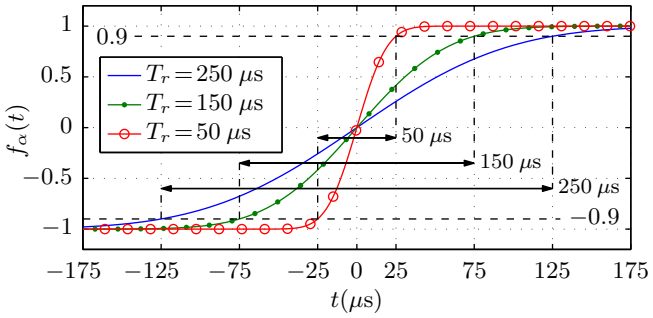

Fig. 2. Sigmoidal function $f_\alpha(t)$ for different rise times T_r.

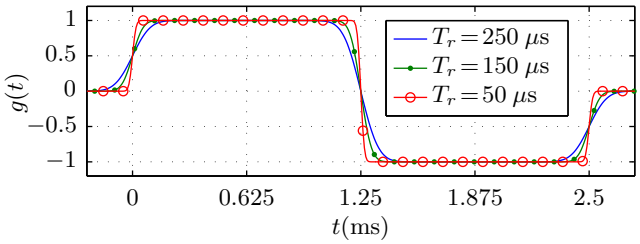

Fig. 3. Manchester pulse $g(t)$ for different rise times T_r.

As will be seen later, this characteristic is important for obtaining a closed-form expression of the MCRBs of interest. The parameter α allows the signal rise and fall times (both represented by T_r) to be adjusted. For the phase-modulated Cospas-Sarsat signal, the rise time is defined as the time taken by the phase to change from 10% to 90% of the step size [7], i.e., for the sigmoidal function $f_\alpha(t)$ to change its amplitude from -0.9 to 0.9 (Fig. 2). Thus

$$\alpha = \frac{2\,\text{erf}^{-1}(0.9)}{T_r} \approx \frac{2.3262}{T_r} \tag{5}$$

where $\text{erf}^{-1}(\cdot)$ is the inverse error function. The shape of the SAR pulse $g(t)$ is illustrated in Fig. 3 for the minimum ($T_r = 50\ \mu$s), nominal ($T_r = 150\ \mu$s) and maximum ($T_r = 250\ \mu$s) values of the rise time following the system specifications [7].

3. MCRB FOR TOA AND SYMBOL WIDTH

Estimating the TOA is closely related to the accurate knowledge of the symbol width, which varies according to the range allowed for the bit rate, $R_s = 1/T = 400\ \text{bps} \pm 1\%$, in [7]. This section studies the MCRBs for the joint estimation of the unknown parameter vector $\boldsymbol{\lambda} = (T, \tau)^T$ containing TOA and symbol width. The covariance matrix of an estimator of $\boldsymbol{\lambda}$, denoted as $\mathbf{C}_{\widehat{\boldsymbol{\lambda}}}$ (where $\widehat{\boldsymbol{\lambda}} = (\widehat{T}, \widehat{\tau})^T$), satisfies the following inequality [8, 9]

$$\mathbf{C}_{\widehat{\boldsymbol{\lambda}}} - \mathbf{I}_M^{-1}(\boldsymbol{\lambda}) \geq \mathbf{0} \tag{6}$$

where $\geq \mathbf{0}$ means that the matrix is positive semi-definite and $\mathbf{I}_M(\boldsymbol{\lambda})$ is the 2×2 modified Fisher information matrix (MFIM). The elements of the MFIM are classically defined as

$$[\mathbf{I}_M(\boldsymbol{\lambda})]_{ij} = \mathbb{E}_{\mathbf{r},\mathbf{u}}\left[\frac{\partial \ln p(\mathbf{r}|\mathbf{u},\boldsymbol{\lambda})}{\partial \lambda_i}\frac{\partial \ln p(\mathbf{r}|\mathbf{u},\boldsymbol{\lambda})}{\partial \lambda_j}\right] \tag{7}$$

where $\mathbf{r}$ is the vector of coefficients obtained from an orthonormal expansion of $r(t)$, $\mathbf{u} = (A, \nu, \mathbf{b})^T$ is the nuisance parameter vector and $p(\mathbf{r}|\mathbf{u},\boldsymbol{\lambda})$ is the probability density function of the observation vector. The MFIM contains $p(\mathbf{r}|\mathbf{u},\boldsymbol{\lambda})$ instead of $p(\mathbf{r}|\boldsymbol{\lambda})$ in the classical FIM, which is much easier to use. It is usually more convenient to use a formalism based on continuous waveforms. As explained in [10, p. 292], in the limit, as the dimension of $\mathbf{r}$ tends to infinity, $p(\mathbf{r}|\mathbf{u},\boldsymbol{\lambda})$ can be replaced by

$$p(\mathbf{r}|\mathbf{u},\boldsymbol{\lambda}) = \exp\left[-\frac{1}{2N_0}\int_{T_0}|r(t)-s(t)|^2 dt\right] \tag{8}$$

where T_0 is the signal duration. After replacing (8) in (7), following the derivations of [6], the MFIM elements can be written as

$$[\mathbf{I}_M(\boldsymbol{\lambda})]_{ij} = \frac{1}{N_0}\mathbb{E}_{\mathbf{u}}\left[\int_{T_0} I_t(\lambda_i,\lambda_j)\,dt\right] \tag{9}$$

where

$$I_t(\lambda_i,\lambda_j) = \frac{\partial s_R(t)}{\partial \lambda_i}\frac{\partial s_R(t)}{\partial \lambda_j} + \frac{\partial s_I(t)}{\partial \lambda_i}\frac{\partial s_I(t)}{\partial \lambda_j}. \tag{10}$$

The next part of this section computes the off-diagonal element of the MFIM for $\boldsymbol{\lambda} = (T, \tau)^T$. Using the notations $\phi_\nu(t) = 2\pi\nu t$ and $\phi_g(t) = \beta\sum_{n=0}^{N-1} b_n\, g(t - nT - \tau)$, $s_R(t)$ and $s_I(t)$ can be expressed as

$$s_R(t) = A\cos[\phi_\nu(t) + \phi_g(t)] \tag{11}$$

$$s_I(t) = A\sin[\phi_\nu(t) + \phi_g(t)]. \tag{12}$$

Thus the integrand $I_t(T,\tau)$ in (9) can be written

$$I_t(T,\tau) = A^2\frac{\partial\phi_g(t)}{\partial T}\frac{\partial\phi_g(t)}{\partial \tau}. \tag{13}$$

Computing the partial derivatives of $\phi_g(t)$ with respect to T and τ yields

$$I_t(T,\tau) = A^2\beta^2\sum_{n=0}^{N-1}\sum_{m=0}^{N-1} b_n b_m p_{n,T}(t)p_{m,\tau}(t) \tag{14}$$

where $p_{n,T}(t) = \partial g(t - nT - \tau)/\partial T$ and $p_{m,\tau}(t) = \partial g(t - mT - \tau)/\partial\tau$. Since the symbols b_n and b_m are independent for $n \neq m$, $\mathbb{E}[b_n b_m^*] = \delta_{nm}$ (where δ_{nm} is the Kronecker delta), hence

$$[\mathbf{I}_M(\boldsymbol{\lambda})]_{12} = \frac{A^2\beta^2}{N_0}\sum_{n=0}^{N-1}\int_{T_0} p_{n,T}(t)\,p_{n,\tau}(t)\,dt. \tag{15}$$

The integral $\int_{T_0} p_{n,T}(t)\,p_{n,\tau}(t)dt$ (denoted as $E_{p,n}$) can be evaluated in the frequency domain by considering a bandwidth B and the sigmoidal Manchester pulse

$$E_{p,n} = \int_{T_0} p_{n,T}(t)\,p^*_{n,\tau}(t)dt \tag{16}$$

$$= \int_{-B/2}^{B/2} P_{n,T}(f)P^*_{n,\tau}(f)df. \tag{17}$$

Straightforward computations and approximations detailed in the Appendix (see (39)) lead to

$$E_{p,n} = \frac{3\alpha}{\sqrt{2\pi}}(2n+1) \tag{18}$$

for $B \geq \alpha\sqrt{2}$. After replacing the expression of $E_{p,n}$ in (15), the off-diagonal element of the MFIM can be written

$$[\mathbf{I}_M(\boldsymbol{\lambda})]_{12} = \frac{3}{\sqrt{2\pi}}\left(\frac{\alpha A^2\beta^2}{N_0}\right)N^2 \tag{19}$$

for $B \geq \alpha\sqrt{2}$. The diagonal elements of the MFIM are obtained in a similar fashion by setting $\lambda_i = \lambda_j = T$ for $[\mathbf{I}_M(\boldsymbol{\lambda})]_{11}$ and $\lambda_i = \lambda_j = \tau$ for $[\mathbf{I}_M(\boldsymbol{\lambda})]_{22}$. The MFIM matrix $\mathbf{I}_M(\boldsymbol{\lambda})$ can finally be expressed as

$$\mathbf{I}_M(\boldsymbol{\lambda}) = 3\sqrt{\frac{2}{\pi}}\left(\frac{\alpha A^2\beta^2}{N_0}\right)\begin{bmatrix}\frac{N^3}{3} & \frac{N^2}{2}\\ \frac{N^2}{2} & N\end{bmatrix}. \tag{20}$$

The closed-form expression (20) can be used to derive the modified Cramér-Rao bounds for the joint estimation of (T,τ), for the estimation of τ (known T) and for the estimation of T (known τ). The results are summarized in the next sections.

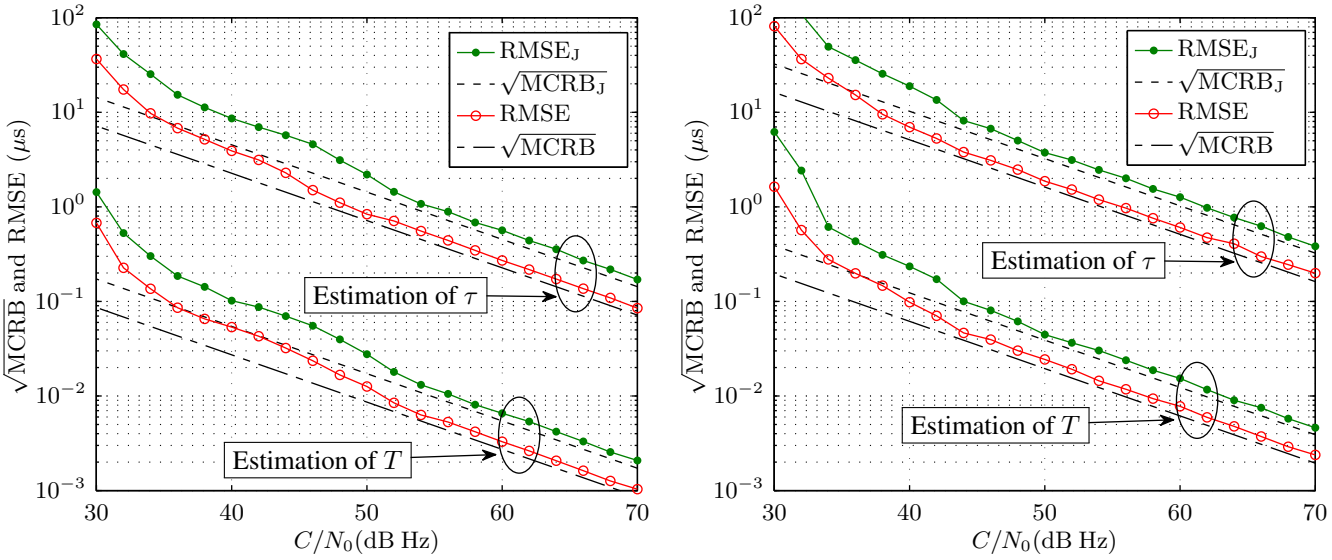

(a) $T_r = 50$ μs. (b) $T_r = 250$ μs.

Fig. 4. Performances for TOA and symbol width estimation for (a) minimum and (b) maximum rise times allowed on the SAR system.

3.1. Joint estimation of (T, τ)

The diagonal elements of the matrix $\mathbf{I}_M^{-1}(\boldsymbol{\lambda})$ define the MCRBs of T and τ for the joint estimation of these two parameters. The inverse of (20) can be computed easily, leading to

$$\mathbf{I}_M^{-1}(\boldsymbol{\lambda}) = 4\sqrt{\frac{\pi}{2}}\left(\frac{N_0}{\alpha A^2 \beta^2 N^3}\right)\begin{bmatrix} 1 & -\frac{N}{2} \\ -\frac{N}{2} & \frac{N^2}{3} \end{bmatrix}. \tag{21}$$

Hence, with $B \geq \alpha\sqrt{2}$, the following results are obtained

$$\text{MCRB}_J(T) = 4\sqrt{\frac{\pi}{2}}\frac{1}{\alpha\beta^2\left(\frac{C}{N_0}\right)N^3}, \tag{22}$$

$$\text{MCRB}_J(\tau) = \frac{4}{3}\sqrt{\frac{\pi}{2}}\frac{1}{\alpha\beta^2\left(\frac{C}{N_0}\right)N} \tag{23}$$

where $C = A^2$ and the index J denotes joint estimation. These latter expressions show that a higher carrier-to-noise-density ratio (C/N_0) provides more accurate results, which is usually expected for minimum variance bounds. Also, increasing α, i.e., reducing the rise time, or increasing β (the amplitude of the phase-modulated pulse), produces more abrupt pulses and thus better estimation results. Finally, the MCRB for T is inversely proportional to N^3, which is a classical property already obtained for other symbol width bounds [11, 12]. The MCRB for τ is inversely proportional to N which is also a classical result (see similar TOA bounds derived in [6, 13]).

3.2. Estimation of T for known τ

Inverting $[\mathbf{I}_M(\boldsymbol{\lambda})]_{11}$ in (20) gives the modified bound for any unbiased estimator of T for a known value of τ

$$\text{MCRB}(T) = \sqrt{\frac{\pi}{2}}\frac{1}{\alpha\beta^2\left(\frac{C}{N_0}\right)N^3} \tag{24}$$

for $B \geq \alpha\sqrt{2}$. By comparing this result with (22), one can appreciate the loss of performance regarding the estimation of T when τ is estimated. More precisely,

$$\text{MCRB}_J(T) = 4\,\text{MCRB}(T). \tag{25}$$

3.3. Estimation of τ for known T

Inverting $[\mathbf{I}_M(\boldsymbol{\lambda})]_{22}$ in (20) gives the modified bound for any estimator of τ when T is known

$$\text{MCRB}(\tau) = \frac{1}{3}\sqrt{\frac{\pi}{2}}\frac{1}{\alpha\beta^2\left(\frac{C}{N_0}\right)N} \tag{26}$$

for $B \geq \alpha\sqrt{2}$. By comparing this value with (23), one can appreciate the loss of performance regarding the estimation of τ when T is estimated. The following result can be obtained

$$\text{MCRB}_J(\tau) = 4\,\text{MCRB}(\tau) \tag{27}$$

as will be verified in the next Section devoted to simulation results.

4. SIMULATION RESULTS

This section compares the MCRBs for the joint estimation of the TOA and symbol width estimation with mean-square errors (MSE) computed from $N_m = 1000$ Monte Carlo runs (i.e. $N_m = 1000$ simulated distress messages), using the proposed signal model. The estimation of T and τ is carried out with the so-called resampling method inspired by the works conducted in [14] exploiting the cyclic correlation of the SAR signal and the symmetry of the pulse. More precisely, the integration of a sequence of Manchester pulses leads to a sum of triangular functions located at time instants kT, $k = 1, \ldots, N$, which are concave or convex depending on the information bit b_n of each symbol. This integration is performed for different values of τ and T within a pre-specified grid whose resolution is chosen sufficiently fine (40 values for T and 40 values for τ) to ensure good estimation performance. Finally, the value of $\boldsymbol{\lambda} = (T, \tau)^T$ maximizing a *contrast function* provided in [14] is used to build $\widehat{\boldsymbol{\lambda}}$.

The simulation parameters used in this paper are displayed in Table 1 and correspond to the system specifications given in [7]. Figs. 4(a) and 4(b) compare the square roots of the MCRBs with the root mean square errors (RMSE) of τ and T for $T_r = 50$ μs and $T_r = 250$ μs, respectively. Note that these values of T_r correspond to the minimum and the maximum values allowed for the SAR signal. The RMSEs of the estimates are close to the corresponding bounds, illustrating the good performance of the estimators. For lower C/N_0, we notice a threshold effect, as it is nearly

Table 1. Simulation parameters.

Parameter	Symbol	Value	Unit
Symbol rate	R_s	404	symbols/s
Number of symbols	N	144	symbols
Modulation index	β	1.1	radians
Bandwidth	B	$\alpha\sqrt{2}$	Hz
Number of messages	N_m	1000	messages

always exhibited by nonlinear estimators [8]. Moreover, more accurate estimations are obtained for a shorter rise time (corresponding to Fig. 4(a)), as expected. These curves can be used to assess a given system performance for different values of the system parameters, such as the number of symbols N. For instance, in order to improve the performance of the next-generation distress beacons, the message length could be adjusted accordingly [15].

5. CONCLUSION

This paper derived modified Cramér-Rao bounds for the symbol-width and the time of arrival of a search and rescue signal model based on smooth transitions. This model is interesting to describe the smooth rise time and fall time of signals received by medium Earth orbit satellites that might be used for the future generation of distress beacons. The obtained bounds provide a reference for the mean square errors of estimators and can be used to adjust some system parameters. Better accuracies can be achieved, e.g., by augmenting the number of symbols, or constraining the signal rise and fall times. Future works could be oriented to the estimation of the frequencies of arrival of search and rescue signals, as well as the estimation of the distress beacon position, considering the parameters already estimated.

6. RELATION TO PRIOR WORK

TOA lower bounds are usually defined as a function of spectral second-order moments, e.g. in [16]. However, these bounds can be difficult to interpret. A bound based on derivatives of the pulse shaping function was introduced in [17]. However, the obtained integral-based expression is still difficult to be studied. This paper derives simple closed-form expressions for the modified Cramér-Rao bounds of symbol width and TOA based on a sigmoidal model for the transitions of search and rescue signals. These results are easy to analyze, in particular regarding the effect of the rise time parameter or the value of the model parameters (number of symbols, carrier-to-noise-density ratio and modulation index).

7. APPENDIX

This Appendix derives a closed form expression of $E_{p,n}$ using its expression in the frequency domain. Using (3) and (4), $p_{n,T}(t)$ and $p_{n,\tau}(t)$ and their Fourier transforms can be expressed as

$$p_{n,T}(t) = \frac{\alpha}{\sqrt{\pi}}\Big[(2n+1)e^{-\alpha^2(t-nT-T/2-\tau)^2} - (n+1)e^{-\alpha^2(t-nT-T-\tau)^2} - ne^{-\alpha^2(t-nT-\tau)^2}\Big] \tag{28}$$

$$p_{n,\tau}(t) = \frac{\alpha}{\sqrt{\pi}}\Big[2e^{-\alpha^2(t-nT-T/2-\tau)^2} - e^{-\alpha^2(t-nT-T-\tau)^2} - e^{-\alpha^2(t-nT-\tau)^2}\Big] \tag{29}$$

$$P_{n,T}(f) = e^{-\frac{\pi^2 f^2}{\alpha^2}} e^{-j2\pi f(nT+\tau)} \times \big[(2n+1)e^{-j\pi fT} - (n+1)e^{-j2\pi fT} - n\big] \tag{30}$$

$$P_{n,\tau}(f) = e^{-\frac{\pi^2 f^2}{\alpha^2}} e^{-j2\pi f(nT+\tau)} \times \big[2e^{-j\pi fT} - e^{-j2\pi fT} - 1\big]. \tag{31}$$

Thus,

$$P_{n,T}(f)P^*_{n,\tau}(f) = e^{-\frac{2\pi^2 f^2}{\alpha^2}}\big[6n+3-(4n+1)e^{j\pi fT} - (4n+3)e^{-j\pi fT} + ne^{j2\pi fT} + (n+1)e^{-j2\pi fT}\big]. \tag{32}$$

As the imaginary part of (32) is composed of odd functions, its integral on the symmetric interval $[-B, B]$ reduces to zero, hence

$$E_{p,n} = (2n+1)\int_{-B/2}^{B/2} e^{-\frac{2\pi^2 f^2}{\alpha^2}}[3 - 4\cos(\pi fT) + \cos(2\pi fT)]df. \tag{33}$$

Using the following identity [18, p. 108]

$$\int e^{-(ax^2+2bx)}dx = \frac{1}{2}\sqrt{\frac{\pi}{a}}\, e^{\frac{b^2}{a}}\,\mathrm{erf}\left(x\sqrt{a} + \frac{b}{\sqrt{a}}\right) \tag{34}$$

with $a \neq 0$, and considering the interval $f \in \big[-\frac{B}{2}, \frac{B}{2}\big]$,

$$\int_{-\frac{B}{2}}^{\frac{B}{2}} e^{-\frac{2\pi^2 f^2}{\alpha^2}}\cos(2\pi fx)df = \frac{\alpha e^{-\frac{x^2\alpha^2}{2}}}{\sqrt{2\pi}}\mathrm{Re}\left[\mathrm{erf}\left(\frac{\pi B + jx\alpha^2}{\alpha\sqrt{2}}\right)\right] \tag{35}$$

the integral in (33) is evaluated as

$$E_{p,n} = (6n+3)\frac{\alpha}{\sqrt{2\pi}}\,\mathrm{Re}\left[\mathrm{erf}\left(\frac{\pi B}{\alpha\sqrt{2}}\right)\right] - (8n+4)\frac{\alpha}{\sqrt{2\pi}}e^{-\frac{T^2\alpha^2}{8}}\mathrm{Re}\left[\mathrm{erf}\left(\frac{\pi B + j(T/2)\alpha^2}{\alpha\sqrt{2}}\right)\right] + (2n+1)\frac{\alpha}{\sqrt{2\pi}}e^{-\frac{T^2\alpha^2}{2}}\,\mathrm{Re}\left[\mathrm{erf}\left(\frac{\pi B + jT\alpha^2}{\alpha\sqrt{2}}\right)\right]. \tag{36}$$

At this point, an approximation is used. Due to the exponential envelope in (32), when considering a bandwidth $B = \alpha\sqrt{2}$, it occurs that $\mathrm{erf}(\pi) = 99.9991\%$ of the integral of the envelope is comprised in this bandwidth:

$$\int_{-B/2}^{B/2} e^{-\frac{2\pi^2 f^2}{\alpha^2}}df = \frac{\alpha}{\sqrt{2\pi}}\,\mathrm{erf}\left(\frac{B\pi}{\alpha\sqrt{2}}\right)\Bigg|_{B=\alpha\sqrt{2}} = \frac{\alpha\,\mathrm{erf}(\pi)}{\sqrt{2\pi}} \tag{37}$$

Hence, the result obtained for $B = \infty$ can be used as an approximation to the case of interest when the condition $B \geq \alpha\sqrt{2}$ is met. Also, considering the rise and fall times of the modulated waveform, and the symbol width specifications, the following result can be obtained

$$e^{-\frac{T^2\alpha^2}{8}}\Big|_{\substack{T_r=250\ \mu\mathrm{s}\\ T=0.0025\ \mathrm{s}}} = 4.2163\times 10^{-30} \tag{38}$$

As a consequence, the two terms in (36) $e^{-\frac{T^2\alpha^2}{2}}$ and $e^{-\frac{T^2\alpha^2}{8}}$ can be neglected leading to the final result

$$E_{p,n} = \frac{3\alpha}{\sqrt{2\pi}}(2n+1), \quad B \geq \alpha\sqrt{2}. \tag{39}$$

8. REFERENCES

[1] Cospas-Sarsat Council, "Introduction to the Cospas-Sarsat system," Tech. Rep. G.003, Issue 6, COSPAS-SARSAT, Oct. 2009.

[2] A. Mehta, "The Int. Cospas-Sarsat Programme: Taking the "search" out of search and rescue," in *Proc. of the Marine Safety & Security Council*, 2011, vol. 68, pp. 12–15.

[3] P. C. Gomez, C. F. Prades, J. A. F. Rubio, G. S. Granados, and I. Stojkovic, "Design of Local User Terminals for Search and Rescue Systems with MEO Satellites," in *Proc. of the 2nd ESA Workshop on Satellite Navigation User Equipment Technologies (NAVITEC)*, Noordwijk, The Netherlands, Dec. 2004, ESA/ESTEC.

[4] A. M. Reza and M. Doroodchi, "Cramér-Rao lower bound on locations of sudden changes in a steplike signal," *IEEE Trans. Signal Process.*, vol. 44, no. 10, pp. 2551–2556, Oct. 1996.

[5] J. Y. Tourneret, A. Ferrari, and A. Swami, "Cramér-Rao lower bounds for change points in additive and multiplicative noise," *Signal Process., EURASIP*, vol. 84, no. 7, pp. 1071–1088, July 2004.

[6] A. N. D'Andrea, U. Mengali, and R. Reggiannini, "The modified Cramér-Rao bound and its application to synchronization problems," *IEEE Trans. Commun.*, vol. 42, no. 234, pp. 1391 –1399, Feb. 1994.

[7] Cospas-Sarsat Council, "Specification for Cospas-Sarsat 406 MHz distress beacons," Tech. Rep. T.001, Issue 3, Revision 12, COSPAS-SARSAT, Oct. 2011.

[8] S. M. Kay, *Fundamentals of Statistical Signal Processing: Estimation theory*, Prentice Hall, 1993.

[9] F. Gini, R. Reggiannini, and U. Mengali, "The modified Cramér-Rao bound in vector parameter estimation," *IEEE Trans. Commun.*, vol. 46, no. 1, pp. 52–60, Jan. 1998.

[10] J. G. Proakis and M. Salehi, *Digital Communications*, McGraw Hill, Boston, 5th edition, 2008.

[11] Y. T. Chan, J. W. Plews, and K. C. Ho, "Symbol rate estimation by the wavelet transform," in *Int. Conf. Circuits and Systems*, June 1997, vol. 1, pp. 177–180.

[12] Z.-M. Deng and Y. Liu, "Modified Cramér-Rao lower bound for symbol width estimation from a phase-shift-keying signal," *J. on Commun.*, vol. 30, no. 2, pp. 117–121, Sept. 2009.

[13] M. Moeneclaey, "On the true and the modified Cramér-Rao bounds for the estimation of a scalar parameter in the presence of nuisance parameters," *IEEE Trans. Commun.*, vol. 46, no. 11, pp. 1536 –1544, Nov. 1998.

[14] S. Houcke, A. Chevreuil, and P. Loubaton, "Blind equalization - Case of an Unknown Symbol Period," *IEEE Trans. Signal Process.*, vol. 51, no. 3, pp. 781 – 793, March 2003.

[15] Cospas-Sarsat Council, "Cospas-Sarsat 406 MHz MEOSAR Implementation Plan," Tech. Rep. R.012, Issue 1, Revision 7, COSPAS-SARSAT, Oct. 2011.

[16] D. Dardari, M. Luise, and E. Falletti, *Satellite and Terrestrial Radio Positioning Techniques: A signal processing perspective*, Elsevier Science, 2011.

[17] A. Masmoudi, F. Bellili, S. Affes, and A. Stephenne, "Closed-form expressions for the exact Cramér-Rao bounds of timing recovery estimators from BPSK and square-QAM transmissions," in *Proc. Int. Conf. on Commun.*, Kyoto, Japan, June 2011, pp. 1–6.

[18] I. S. Gradshteyn, I. M. Ryzhik, A. Jeffrey, and D. Zwillinger, *Table of Integrals, Series and Products*, Academic Press, 2007.